Simulation of Flow and Chemical Reactions in a Claus Sulfur Converter

Habib Daoud Zughbi* and Shaikh Abdur Razzak

Department of Chemical Engineering, King Fahd University of Petroleum & Minerals, Dhahran, 31261 Saudi Arabia

Three-dimensional computational fluid dynamics (CFD) models were developed to investigate the flow distribution and chemical reactions in a partially packed vessel similar to a catalytic sulfur converter used to sweeten sour gas, known as a Claus converter. A gas feed enters the vessel and reacts over the catalyst before leaving as products. Simulations of the flow in a Claus converter showed that the packed bed acts as a good flow distributor. However, some fluctuations of flow were observed in the packed bed, especially in the zones corresponding to the incoming feed jet impingement locations. Near the outlet of the bed, the flow becomes significantly better distributed. The chemical reactions were simulated using a finite rate model. Results of the complete CFD model (including flow, chemical reactions, and heat transfer) of each of two Claus converters placed in series showed good agreement with the available industrial data. The numerically predicted conversion matched the available value closely, and so did the detailed composition of the gas leaving each of the three converters. The predicted and measured values of the temperature also showed good agreement.

Introduction

In the chemical and petrochemical industry, packed beds can be found in diverse applications. They are used as reaction, separation, and purification units. Fluid flow plays a significant role in these operations. Reaction engineering crucially depends on the fluid dynamics and mixing occurring in an industrial reactor. Therefore, a good understanding of flow behavior and distribution is often crucial for the proper design and operation of equipment such as packed and unpacked reactors. However, detailed knowledge of the flow distribution and the chemical reactions is rather limited mainly because most vessels are operated at high temperature and pressure, which makes the measurement of velocities a difficult task.

Computational fluid dynamics (CFD) can predict the detailed flow in a reactor under different geometric and operating conditions. Design elements that need to be considered when dealing with packed beds include pressure drop, flow maldistribution, interfacial and intraparticle gradients, and the effect of the catalyst characteristics on the process or hydrodynamic design.

Although many flow problems in unpacked and packed vessels have been investigated experimentally and numerically, there does not seem to be many published references that deal with flow distribution in large industrial vessels. Most of the research in this area has been concentrated on some theoretical model developments, generally on a very small scale.

The vessel simulated in the present study is similar to an industrial Claus converter. This converter is a horizontal cylinder, 18.2 m long and 4.9 m in diameter. It has three inlets and one outlet. Each inlet is 0.6 m in diameter while the outlet diameter is 1 m. A schematic diagram of such a converter is shown in Figure 1. A gas feed enters the vessel at a velocity of 57 m/s. The vessel contains a 1.2 m high catalyst bed placed about 1.4 m above the bottom of the converter. The main reaction that takes place over the catalyst bed is known as the Claus reaction, where hydrogen sulfide reacts with sulfur dioxide to produce elemental sulfur and water vapor.

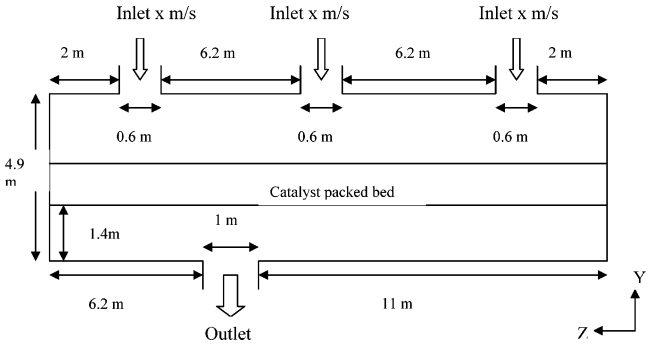

Figure 1. Schematic diagram of a Claus converter used in the present investigations.

Though the geometry and operating conditions of the vessel appear to be simple, they contribute to flow maldistribution, thereby reducing the overall efficiency of the vessel. In this study, the flow, chemical reactions, and thermal effects in each of two industrial catalytic Claus converters placed in series are simulated. "In series" means that the product gas leaving the first converter is fed into the second converter.

Many oil refiners and gas processors use the Claus process in order to convert much of the H_2S to elemental sulfur in order to meet environmental regulations. The Claus sulfur recovery process includes a furnace and converters. The furnace side has been the topic of much more research compared to the Claus converters. The lifetime of the catalyst used in a Claus converter varies from about 2 years to more than 8 years, depending on the feed gas composition, especially the feed contents of benzene, toluene, and xylene (BTX). BTX are known to reduce the lifetime of a Claus catalyst. This study

* To whom correspondence should be addressed. E-mail: hdzughbi@kfupm.du.sa.

10.1021/ie050412m CCC: $30.25
Published on Web 11/02/2005

aims to investigate the flow in a partially packed Claus converter. It also aims at incorporating the chemical reactions within the flow model and at comparing the numerical results with available experimental data. The CFD model could be used in future studies to further investigate ways of ensuring better utilization of all the catalyst in a Claus converter, thus leading to a longer lifetime of the catalyst.

Flow through Packed Beds. CFD can be used to model a wide variety of flows through porous media, including flow through packed beds, perforated plates, flow distributors, and tube banks. Typically, a porous media model incorporates an empirically determined flow resistance in a region of the model defined as porous. A porous media model is nothing more than an added momentum sink in the governing momentum equations.

A number of early studies showed that reactions and radial heat transfer can only be modeled correctly if the nonuniformities of the bed structure are properly considered. Therefore, over the years, a number of studies investigated the radial variation of the axial gas velocity in packed beds. These studies included axial velocity measurements at various radial positions, measurement of radial porosity profiles,[1] and modeling of the radial variation of axial velocity. It was noted, however, that, in industrial packed beds, some nonuniformities, either due to the presence of internal structures or due to irregular gas inlet design, could cause the flow to not be one-dimensional and the gas velocity to vary in both radial and axial directions.[2] Such a two-dimensional flow is called "nonparallel" flow in the literature. Hence, for industrial applications of packed beds, it is certainly important to be able to effectively model the nonparallel gas flow.

The vectorized Ergun equation model is based on the assumption that a packed bed can be treated as a continuum. The model utilizes the empirical Ergun equation,[3] which holds well for the overall pressure drop in the macroscopic beds with unidirectional flow, for an infinitesimal length of the bed and applied in the direction of the flow. A number of investigators utilized this method to model two- and three-dimensional flow in packed beds.

The equations of motion model, in principle, solves the mass and momentum conservation equations for the flowing phase provided the solid boundaries are precisely specified. By employing the effective viscosity as an adjusting factor, Ziolkowska and Ziolkowski[4] and Bey and Eigenberger[5] developed a mathematical model for the interstitial velocity distribution.

Fluid flow between particles in packed beds is characterized by a random packing geometry, high turbulence, and strong velocity fluctuations.[6] Any realistic flow model must, therefore, be based on some averaging assumptions. One generally accepted procedure is to assume angular symmetry (in the case of a cylindrical coordinate system) of the flow profile and to consider a continuous distribution of the void fraction in the packing. Then, any fluid flow will create continuously distributed interstitial velocity. The flow can be described by the Navier−Stokes equations if additional terms of fluid−particle interactions are incorporated. The fluid−particle interactions may be described by the Ergun pressure correlation, and the fluid wall friction is separately taken into account. This allows the application of a no-slip boundary condition at the wall where the void fraction approaches unity. The fluid wall friction affects the flow profile only in the immediate vicinity of the wall, whereas inside the packing the Ergun pressure drop, describing fluid−particle interaction, is far dominating.

Vortmeyer and Schuster[7] used this variation approach to evaluate the steady two-dimensional velocity profiles for an isothermal incompressible flow in rectangular and cylindrical packed beds. They used the continuity equations, Brinkman's equation, and a semiempirical expression for the radial porosity profile in the packed bed to compute these profiles. Their results showed that a significant preferential wall flow occurs in cases where the ratio of the channel diameter to the particle diameter becomes significantly small. Although their study was done for an idealized solution, it has laid the foundation for more detailed studies. The momentum equations for interstitial velocity had been used assuming a laminar viscosity. Bey and Eigenberger[5] used the increased "turbulent viscosity" which accounts for highly turbulent interstitial flow. They took measurements outside the fixed bed behind a monolith as the fluid shifts from the region near the wall to the center. When the comparison was carried out between measured velocity profiles outside the bed and simulations, they concluded that these changes have to be taken into account. These researchers have used a two-dimensional model containing the continuity equation and the momentum balance equations in the radial and axial directions. The momentum balances are composed of the Ergun equation and of shear stress and inertia effects.

In this investigation, the approach of Bey and Eigenberger[5] is used, but model equations are for a Cartesian coordinate system instead of the cylindrical system used by them. The pressure drop in the packing is evaluated by the well-established correlation of the Ergun equation wherein factors determining the (energy loss) pressure drop in packed beds should be considered. These factors are (1) the rate of fluid flow, (2) the viscosity and density of the fluid, (3) the closeness and orientation of the packing, and (4) the size, shape, and surface of the particles. The first two variables concern the fluid, while the last two deal with the solids. In this investigation, the first two variables have been considered for modeling the pressure drop through the packed bed, while the values of the other two factors are assumed to remain constant.

Chemical reactions have also been recently incorporated in CFD studies. Kuipers and Van Swaaij[8] reviewed CFD studies with chemical reactions. Magnussen and Hjertager[9] presented a mathematical model of turbulent combustion. Jiang et al.[10,11] carried out CFD studies of single phase and multiphase flows in packed bed reactors.

From the above literature review, it can be concluded that the importance of the uniform flow distribution had been recognized for a long time, but all the investigations were attempted for lab scale models and there is a scarcity of data for large industrial scale vessels such as the one considered in this investigation. The $\kappa-\epsilon$ turbulence model is used for turbulence modeling. Finally, the modified Ergun equation is used for analyzing flow through packed beds.

Mathematical Formulation. The numerical simulation of flow in a vessel involves specifying the governing conservation equations, using an appropriate tur-

bulence model, and specifying the proper boundary and initial conditions.

The flow in a packed reactor is classified as a single phase flow. The simulation of flow in the Claus converter is carried out under steady-state and nonisothermal conditions. The governing equations for the nonisothermal gas flow in a packed bed are those of the mass, momentum, and energy conservation.

The steady-state continuity equation for an incompressible fluid in the packed beds region is

$$0 = \nabla\cdot(\epsilon\vec{v}) \tag{1}$$

where the bed porosity ϵ and the velocity v are assumed to be continuously varying functions.

The above equation is applicable to flow in the packed part of the vessel. In the unpacked parts, the value of the porosity, ϵ, is 1 and the above equation becomes

$$\nabla\cdot\vec{v} = 0 \tag{2}$$

The stationary momentum balances are formulated according to Bey and Eigenberger[5] as

$$0 = -\rho[\nabla\epsilon\vec{v}\vec{v}] - \nabla p + \mu\nabla^2\epsilon\vec{v} + \epsilon\rho\vec{g} + \vec{S} \tag{3}$$

It should be noted that the gas flow is assumed to be incompressible. This is a reasonable assumption given that most of the feed to a Claus converter is nonreactive gases, mainly nitrogen and carbon dioxide, and that a limited change in temperature and a small change in the number of moles occur in the Claus reaction.

Similar to the case of continuity, the above equation is applicable for the flow in the packed part of the vessel. For the unpacked zones, the value of ϵ becomes 1.

The term $\vec{S}$ contains other model-dependent source terms. At the catalyst bed,

$$\vec{S} = -\left(\frac{\mu}{\alpha}\nu_i + C_2\frac{1}{2}\rho\left|\nu_i\right|\nu_i\right) \tag{4}$$

where α is the permeability and C_2 is the inertial resistance factor. From the Ergun equation, which is a semiempirical correlation applicable over a wide range of Reynolds numbers and for many types of packing, α and C_2 can be represented by

$$\alpha = \frac{D_p^{\,2}}{150}\frac{\epsilon^3}{(1-\epsilon)^2} \tag{5}$$

$$C_2 = \frac{3.5}{D_p}\frac{(1-\epsilon)}{\epsilon^3} \tag{6}$$

where ϵ is the bed porosity and D_p is the diameter of a catalyst particle. In this model, the bed porosity and catalyst diameter were assumed to be 0.5 and 0.0018 m, respectively. Typical values of bed porosity range between 0.4 and 0.5.

Gravitational body forces are represented by way of sources of momentum in the equations for each of the three velocity components. Such sources are specified in a way that ensures the multiplication of the acceleration due to gravity by the mass of the phase in the velocity cell, which results in the source being set to the force acting on the velocity cell. The effects of the body forces in the present simulations may not be great, but the corresponding terms were left in for the sake of completeness.

The energy equation in porous media is the standard transport equation with modifications to the conduction flux and transient terms only. The steady-state energy equation is as follows:

$$\nabla\cdot(\vec{v}(\rho_f E_f + p)) = \nabla\cdot[k_{eff}\nabla T - (\sum_i h_i J_i) + (\bar{\bar{\tau}}\cdot\vec{v})] + S_f^h \tag{7}$$

where E_f is the total energy, k_{eff} is the effective thermal conductivity of the medium, h is the sensible energy, J is the diffusion flux, and S_f^h is the fluid enthalpy source term. S_f^h includes the heat of chemical reaction and any other volumetric heat sources. The effective thermal conductivity is the summation of molecular and turbulent conductivities.

For the unpacked part of the vessel, the standard energy equation is solved.

$$\nabla\cdot(\vec{v}(\rho E + p)) - \nabla\cdot[k_{eff}\nabla T - (\sum_i h_i J_i) + (\bar{\bar{\tau}}\cdot\vec{v})] + S_h \tag{8}$$

Initial and Boundary Conditions. In this study, the inlet condition corresponds to the flow conditions. In the CFD package used, defining an inlet condition means specifying the cells through which the fluid is introduced, the velocities (x-, y-, and z-direction), or the pressure (mass flux-specification). An outlet condition refers to the physical conditions at the flow exit. The specification involves the location of cells, which are desired to be kept open, and the exit pressure. For this study, also, a general no-slip condition is imposed on all solid walls.

Partially Packed Reactors. In process industries, packed beds are frequently used as catalytic reactors, filters, or separation processes such as absorption, adsorption, and distillation. Packed beds are extensively used in many petroleum, petrochemical, and biochemical applications. The modified Claus process is used to recover elementary sulfur from hydrogen sulfide present in gases from refineries and natural gases. A wide range of catalysts dedicated to sulfur recovery and based on the Claus process are available. Catalysts provide the necessary sites to catalyze the conversion of H_2S and SO_2 to elemental sulfur. The Claus reaction is

$$2H_2S + SO_2 \rightleftharpoons \frac{3}{n}S_n + 2H_2O \tag{9}$$

where n could be 2, 6, or 8.

In this study, the flow and chemical reactions in a vessel similar to an industrial Claus converter are simulated taking the thermal effects into consideration.

The mixing and transport of chemical species can be modeled by solving conservation equations describing convection, diffusion, and reaction sources for each component species. Multiple simultaneous chemical reactions can be modeled with reactions occurring in the bulk phase (volumetric reactions) and/or on a wall or particle surfaces and in the porous region. The reactions in the Claus converter are surface reactions, and they are best modeled using surface reactions in the CFD model.

The use of surface reactions in the model requires detailed information about all the main and side reactions including diffusion and surface reactions. The heat release due to surface reactions can also be modeled. Other effects including those of the surface mass

transfer, species diffusion effects in the energy equation, and thermal diffusion can also be modeled. Such detailed information about the reactions in a Claus converter is not available in the literature. A thorough search revealed very little information about detailed kinetics.

Since the detailed procedure of handling the chemical reactions was not feasible due to lack of kinetics data, these reactions were simulated using a volumetric reaction model. A volumetric reaction with species transport is handled in FLUENT using the laminar finite rate model. In this model, the effects of turbulent fluctuations are ignored, and the reaction rate is determined by Arrhenius expressions.

Finite Rate Model. The laminar finite rate model computes the chemical source terms using Arrhenius expressions and ignores the effects of turbulent fluctuations. The model is exact for laminar flames but is generally inaccurate for turbulent flames due to highly nonlinear Arrhenius chemical kinetics. The laminar model may, however, be acceptable for combustion with relatively slow chemistry and small turbulent fluctuations, such as supersonic flames. However, the finite rate model is suitable for the type of catalytic reaction where the reaction depends on some extra kinetic energy that is provided by the catalyst. The finite rate model is more suitable to handle the reaction in the present study than the other models available in FLUENT. The choice of the model that is the best for the Claus reaction will be further explained in the next few paragraphs.

The net source of chemical species i due to reaction R_i is computed as the sum of the Arrhenius reaction sources over the N_R reactions that the species participates in:

$$R_i = M_{w,i}\sum_{r=1}^{N_R}\hat{R}_{i,r} \tag{10}$$

where $M_{w,i}$ is the molecular weight of species i and $\hat{R}_{i,r}$ is the Arrhenius molar rate of creation/destruction of species i in reaction r. A reaction may occur in the continuous phase between continuous-phase species only or at wall surfaces resulting in the surface deposition or evolution of a continuous-phase species. Consider the rth reaction written in a general form as follows:

$$\sum_{i=1}^{N} v'_{i,r}M_i \underset{k_{b,r}}{\overset{k_{f,r}}{\rightleftharpoons}} \sum_{i=1}^{N} v''_{i,r}M_i \tag{11}$$

where N is the number of chemical species in the system, $v'_{i,r}$ is the stoichiometric coefficient for reactant i in reaction r, $v''_{i,r}$ is the stoichiometric coefficient for product i in reaction r, M_i is the symbol denoting species i, $k_{f,r}$ is the forward rate constant for reaction r, and $k_{b,r}$ is the backward rate constant for reaction r. Equation 11 is valid for both reversible and nonreversible reactions. For nonreversible reactions, the backward rate constant, $k_{b,r}$, is simply omitted.

The summations in eq 11 are for all chemical species in the system, but only the species that appear as reactants or products will have nonzero stoichiometric coefficients. Hence, species that are not involved in the reaction will drop out of the equation.

The molar rate of creation/destruction of species i in reaction r, $\hat{R}_{i,r}$, is[12]

$$\hat{R}_{i,r} = (v''_{i,r} - v'_{i,r})\left(k_{f,r}\prod_{j=1}^{N_r}[C_{j,r}]^{\eta'_{j,r}} - k_{b,r}\prod_{j=1}^{N_r}[C_{j,r}]^{\eta''_{j,r}}\right) \tag{12}$$

where N_r is the number of chemical species in reaction r, $C_{j,r}$ is the molar concentration of each reactant and product species j in reaction r (kg mol/m^3), $\eta'_{j,r}$ is the forward rate exponent for each reactant and product species j in reaction r (kg mol/m^3), and $\eta''_{j,r}$ is the backward rate exponent for each reactant and product species j in reaction r (kg mol/m^3).

The forward rate constant for reaction r, $k_{f,r}$, is computed using the Arrhenius expression

$$k_{f,r} = A_r T^{\beta_r} e^{-(E_r/RT)} \tag{13}$$

where A_r is the pre-exponential factor (consistent units), β_r is the temperature exponent (dimensionless), E_r is the activation energy for the reaction (J/(kg mol)), and R is the universal gas constant (J/(kg mol K)).

If the reaction is reversible, the backward rate constant for reaction r, $k_{b,r}$, is computed from the forward rate constant using the following relation:

$$k_{b,r} = \frac{k_{f,r}}{K_r} \tag{14}$$

where K_r is the equilibrium constant for the rth reaction, computed from

$$K_r = \exp\left(\frac{\Delta S_r^\circ}{R} - \frac{\Delta H_r^\circ}{RT}\right)\left(\frac{p_{atm}}{RT}\right)^q \tag{15}$$

$$\text{where } q = \sum_{r=1}^{N_R}(v''_{j,r} - v'_{j,r})$$

and p_{atm} denotes atmospheric pressure (101 325 Pa). The term within the exponential function represents the change in the Gibbs free energy, and its components are computed as follows:

$$\frac{\Delta S_r^\circ}{R} = \sum_{i=1}^{N}(v''_{i,r} - v'_{i,r})\frac{S_i^\circ}{R} \tag{16}$$

$$\frac{\Delta H_r^\circ}{RT} = \sum_{i=1}^{N}(v''_{i,r} - v'_{i,r})\frac{h_i^\circ}{RT} \tag{17}$$

where S_i° and h_i° are the standard-state entropy and standard-state enthalpy (heat of formation). These values are specified as properties of the mixture material.

The main objective of the present work is to consider the Claus reaction of the converter, by which sulfur is removed from sour gas. Little information about the kinetics of the Claus reaction is available in the literature. Information about the kinetics of the Claus reaction in a furnace (at a higher temperature than in the converter) is more available in the literature.[13]

The kinetics of the Claus-process manufacturing of elemental sulfur that is used in the model as developed by Abaskuliev et al.[14] is

$$R(C,T) = 7.3919 \times 10^4 \exp\left(\frac{-30594}{8.314T}\right)\frac{T^{1.5}C_{H_2S}C_{SO_2}{}^{0.5}}{(1 + 46.56TC_{H_2O})^2} \quad (18)$$

To apply this kinetics model for the laminar finite rate chemistry in the CFD package, it needs further simplification. In this simplification, the smallest term of the denominator, 1, was removed. Following the simplification, the model becomes

$$R(C,T) = 34.0981 \exp\left(\frac{-30594}{8.3145T}\right)T^{-0.5}C_{H_2S}C_{SO_2}{}^{0.5}C_{H_2O}{}^{-2} \quad (19)$$

The error resulting from the above simplification is calculated using values of temperature and concentrations that are similar to those found in an industrial Claus converter. Suppose the industrial converter temperature $T = 500$ K, $C_{H_2S} = 0.06377$, $C_{SO_2} = 0.06075$, and $C_{H_2O} = 0.04443$. Submitting these data in eqs 18 and 19 it is found that $R(C,T)_1 = -0.1783$ and $R(C,T)_2 = -0.1787$. These values are very close, and the error resulting from the previous simplification is about 0.2%. One can conclude that eq 19 can be used in the present simulations.

Finite Rate Model with Multiple Sulfur Components. The Claus reaction is exothermic at converter temperatures, and the reaction is favored by lower temperatures. Process calculations for a Claus sulfur recovery unit are complicated by the existence of various species of gaseous sulfur (S_2, S_6, and S_8), whose equilibrium concentrations in relation to each other are often not precisely known, and by a number of side reactions involving other feed gas components, such as carbon dioxide (CO_2), hydrocarbons, ammonia (NH_3), carbonyl sulfide (COS), carbon disulfide (CS_2), etc., which take place simultaneously. These equilibrium and composition calculations are usually carried out by a computer using the software package Sulfane. The variation of sulfur vapor composition with the temperature at atmospheric pressure is given by Maddox.[15] The temperature inside the converter lies between 477 and 589 K. From these figures, it is clear that most of the product is S_8 and then S_6, with a very little amount of S_2 produced as a sulfur vapor. The present investigation focuses on these three different products. In this simulation, the side reactions are ignored. Since the compositions of the reactants involved in the side reactions are very small, the effect of these side reactions on the overall Claus reaction is not expected to be significant.

Since the reaction produces S_2, S_6, and S_8, there is a need for a kinetics model for each of these reactions:

$$2H_2S + SO_2 \rightleftharpoons \frac{3}{2}S_2 + 2H_2O \quad (20)$$

$$2H_2S + SO_2 \rightleftharpoons \frac{3}{6}S_6 + 2H_2O \quad (21)$$

$$2H_2S + SO_2 \rightleftharpoons \frac{3}{8}S_8 + 2H_2O \quad (22)$$

Such kinetics models for the reactions producing S_6 and S_8 are not available. The general kinetics model proposed by Abaskuliev[14] was slightly modified to account for the S_2, S_6, and S_8 reaction, as shown in eqs 20−22.

$$R(C,T) = 34.0981 \exp\left(\frac{-30594}{8.3145T}\right)T^{-0.7}C_{H_2S}C_{SO_2}{}^{0.7}C_{H_2O}{}^{-2}C_{S_2}{}^{\circ} \quad (23)$$

$$R(C,T) = 34.0981 \exp\left(\frac{-30594}{8.3145T}\right)T^{-0.5}C_{H_2S}C_{SO_2}{}^{0.7}C_{H_2O}{}^{-2}C_{S_6}{}^{\circ} \quad (24)$$

$$R(C,T) = 34.0981 \exp\left(\frac{-30594}{8.3145T}\right)T^{-0.4}C_{H_2S}C_{SO_2}{}^{0.7}C_{H_2O}{}^{-2}C_{S_8}{}^{\circ} \quad (25)$$

These modifications were done empirically. The results obtained from simulation cases where the above expressions were used are in good agreement with the industrial results.

Flow Distribution in a Claus Converter. In this study, two Claus converters, identical to the one shown schematically in Figure 1 and placed in series, are simulated. The gas product leaving the first converter is fed into the second converter, and the gas product leaving the second converter is fed into the third. In this section, the flow in the first converter, which is typical of any of the three converters, is analyzed. The bed in this case consists of particles with a size of 0.003175 m in diameter. The porosity of the bed is chosen as a fixed value of 0.5. The porosity of catalytic beds such as those used in Claus converters ranges between 0.4 and 0.5. The present work is three-dimensional so the actual flow distribution in the bed from all three directions can be observed.

It should be mentioned that the near wall velocity profile reported by many researchers in the literature including Szekely and Poveromo[16] will not be noticed in the current simulations. This is due to the mesh size. The size of each mesh cell is 0.025 m, while the catalyst particles are 0.003175 m in diameter. This means that every mesh cell covers a large number of particles. The size of the bed is sufficiently large to neglect wall effects, and consequently, a mesh size larger than the particle size in the near wall region is justified.

By closely inspecting the velocity contours in three carefully chosen horizontal planes, one could obtain a clear picture of the flow distribution which may have a direct impact on the degree of conversion of the Claus reactions and consequently on the degree of the catalyst utilization.

Figure 2 shows a plane cut through the inlets and outlet of the Claus converter. Three lines are shown and will be referred to frequently in this and subsequent sections. The line at $y = -0.1$ m is near the top (inlet) of the packed bed, the line at $y = -0.5$ m is near the middle of the bed, and the line at $y = -1$ m is near the bottom of the bed. Figure 3 shows a horizontal plane cut across the converter. Three lines are shown and will be referred to in the following sections. The first is at $x = 0.5$ m from the center of the converter, the second line is at $x = 1.0$ m from the center of the converter, and the third line is $x = 2.0$ m away from the center in the same horizontal $X-Z$ plane. This makes the third line close to the converter wall.

Figure 4 shows the line plots of velocity magnitudes versus position for three different values of the inlet velocity. These plots present the variation of the velocity magnitude along the length of the reactor, i.e., the z axis. The lines are drawn at the position of $y = -0.1$ m, that is, near the inlet of the bed. This central line shown

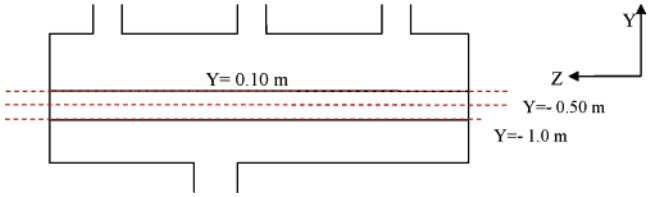

Figure 2. Plane ($y-z$) through the center of the converter showing three y-lines where cuts are frequently taken: $y = 0.1$ m near the top of the packed bed, $y = -0.50$ m near the middle of the bed, and $y = -1.0$ m near the bottom of the bed.

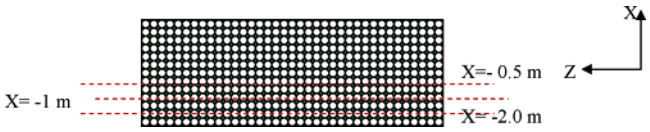

Figure 3. Horizontal $x-z$ plane through the center of the converter showing three y-lines where cuts are frequently taken: $x = -0.5$ m away from the center of the packed bed, $y = -1.0$ m from the center of the bed and the wall, and $x = -2.0$ m from the center of the bed.

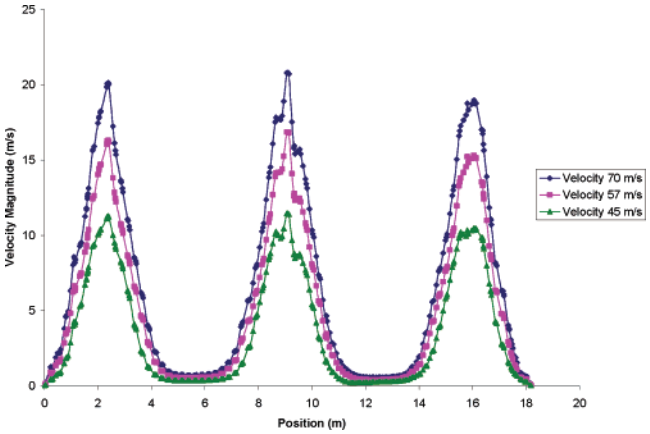

Figure 4. Line plots of the velocity across the bed for different values of the inlet velocity. These plots present the variations of the velocity magnitude along the z-axis near the inlet of the bed at $y = -0.1$ m and $x = 0$ m.

in this plot is created between (0, −0.1, 0) and (0, −0.1, 18.20). These plots show the variation in the velocity more clearly than the contour plots. The velocity variations in the three areas of the jet impingements are much higher compared to those in other areas. The velocities lie between 0.2 and 21 m/s. The flow distribution is similar except for the peak values, which increase as the inlet velocity increases. There are three noticeable peaks in the velocity plots, and they correspond to the incoming jets or to their areas of impingement. These three regions are large and extend almost 4 m in width. The right jet impingement zone is slightly smaller in magnitude than the other two adjacent jets. The middle jet shows the highest velocity magnitudes. However, the velocity in the zones between any two adjacent jets is very low. Using an inlet velocity of 45, 57, or 75 m/s did not have any significant effect on the flow distribution within the converter or within the catalyst bed.

Figure 5 depicts the line plots of the velocity along a line at $y = -0.50$ m and $x = 0$ m, which is near the middle of the packed bed. The velocity magnitudes are found to be much lower than those of the previous figure. These fall between 0.1 and 4.5 m/s. The middle jet zone shows the highest peak compared to the other two jet impingement zones.

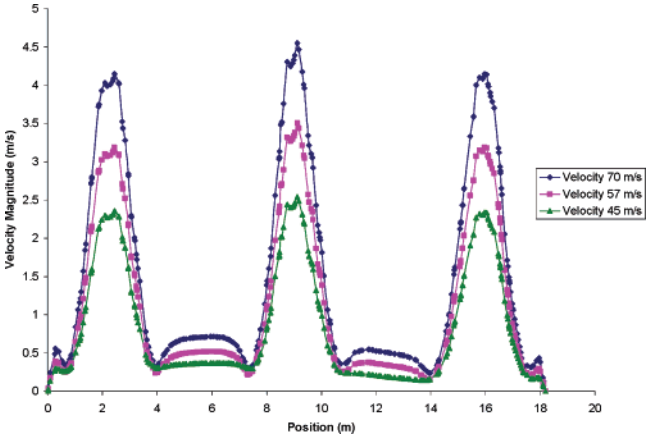

Figure 5. Line plots for different values of the inlet velocity. These plots present the variations of the velocity magnitude along the z-axis near the middle of the bed at $y = -0.50$ m and $x = 0$ m.

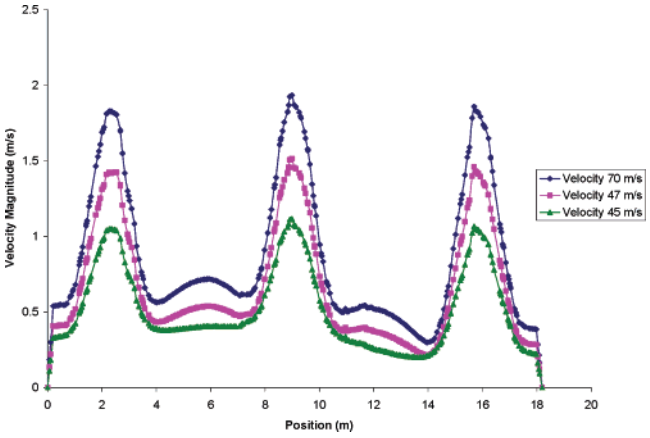

Figure 6. Line plots for different values of the inlet velocity. These plots present the variations of the velocity magnitude along the z-axis near the outlet of the bed at $y = -1.0$ m and $x = 0$ m.

Figure 6 shows the line plots of the velocity along a line located at $y = -1.0$ m and $x = 0$ m. Velocity values range from 0.1 to 2.0 m/s. The interesting phenomenon found in the bed is that the velocity is distributed evenly in low velocity areas. The velocity magnitude in the jet impingements is much closer to those in the adjacent low velocity areas. This means that the packed bed acts as a good distributor; however, significant differences in the values of the velocity are still observed even at the outlet of the bed.

For an inlet velocity of 57 m/s, the average velocity over the horizontal midplane of the converter is 0.54 m/s. Maldistribution is quantified as (actual velocity − average velocity)/average velocity. The maximum value of this number is about 28 near the bed inlet, 5.5 near the middle of the bed, and about 1.8 near the bed outlet.

In the last three line plots, the velocity variations through the center line of the bed, i.e., where $x = 0$ m, were discussed. The velocity variations in the horizontal direction, i.e., the $y-z$ plane of the bed, are now discussed. In Figures 8−10, the velocity variations in the bed at different x positions in a $y-z$ plane are presented. For this purpose, three x positions are considered, as was discussed earlier and shown in Figure 4. These are one line at $x = -0.50$ m, one at $x = -1.0$ m, and one closer to the wall at the $x = -2.0$ m position. All three positions are taken just before the outlet of the bed, which is at $y = -1.0$ m.

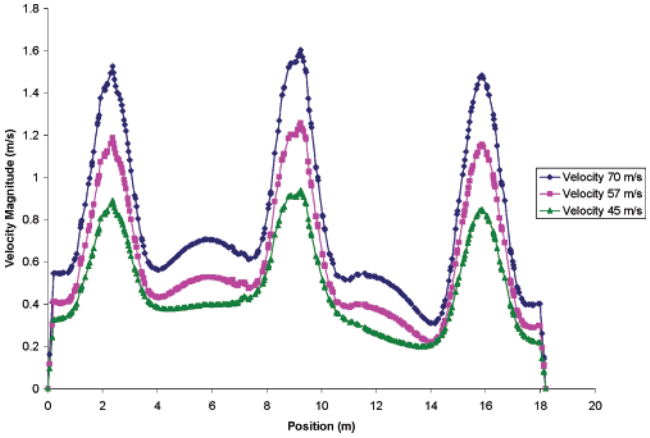

Figure 7. Line plots for different values of the inlet velocity. These plots present the variations of the velocity magnitude along the z-axis at $x = -0.50$ m and $y = -1.0$ m.

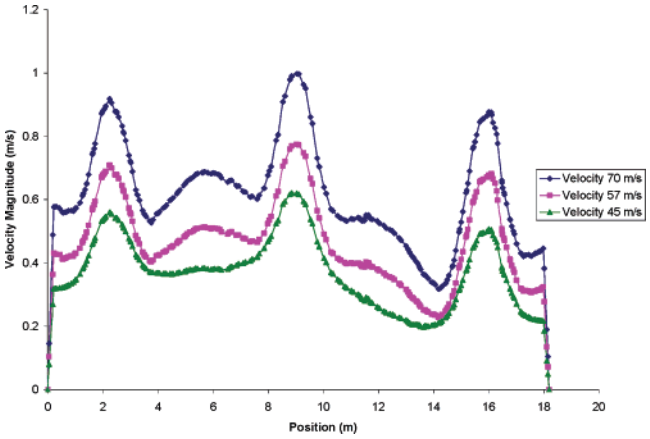

Figure 8. Line plots for different values of the inlet velocity. These plots present the variations of the velocity magnitude along the z-axis at $x = -1.0$ m and $y = -1.0$ m.

Figure 7 shows velocity line plots near the outlet of the bed but 0.5 m from the center in the horizontal direction, i.e., at $x = -0.50$ m and $y = -1.0$ m. This line lies between (−0.50, −1.0, 0) and (−0.50, −1.0, 18.20). The velocity magnitudes are slightly lower than that of the $x = 0$ m line and lie between 0.1 and 1.6 m/s. The difference of velocity magnitudes among the impingement position and its adjacent low velocity zones becomes lower, and it seems that the bed performs as a good flow distributor.

Figure 8 shows the velocity variations in the bed at the point $x = -1.0$ m. This line is taken at a position between the wall and the center of the bed. The line lies between (−1.0, −1.0, 0) and (−1.0, −1.0, −18.20). In this case, a reasonably even distribution of the velocity is observed along the length of the converter and the difference between the maximum and minimum values of the velocities is rather small. The size of the low velocity zones is significantly reduced.

Figure 9 depicts velocity magnitudes along a line very close to the wall, i.e., at $x = -2.0$ m and $y = -1.0$ m. The line lies between (−2.0, −1.0, 0) and (−2.0, −1.0, 18.20). Velocity magnitudes are much lower and lie between 0.1 and 0.75 m/s. No jet impingement effects were observed. On the basis of these observations, it can be concluded that the bed works as a good flow distributor and that the flow becomes rather evenly distributed near the outlet of the bed except in the zones of the impingement of the jets.

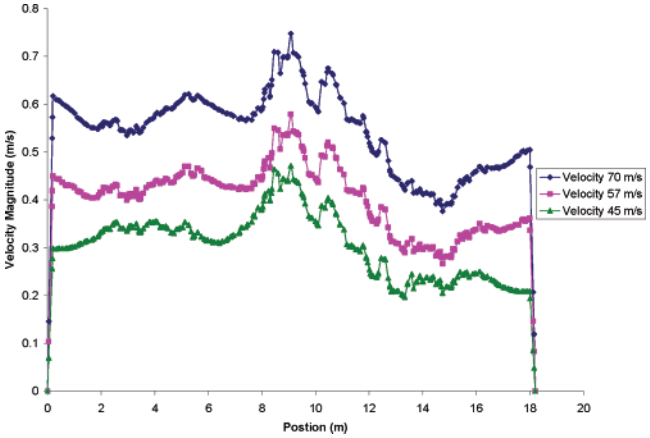

Figure 9. Line plots for different values of the inlet velocity. These plots present the variations of the velocity magnitude along the z-axis at $x = -2.0$ m and $y = -1.0$ m.

The above analysis of the flow distribution inside the Claus converter and especially within the catalyst bed for three different inlet velocities clearly shows that the catalyst bed acts as a flow distributor. However, significant variations in the values of the velocity at different parts of the bed are still observed even near the bed outlet. Varying the inlet velocity from the industrial value of 57 m/s down to 45 m/s and then up to 75 m/s did not improve the flow distribution inside the converter or inside the catalyst bed.

Simulation of Reactions and Heat Transfer in a Claus Converter. Following the discussion of the flow distribution in the first converter, the reactions, degree of conversion, composition of product gas, and temperature profiles in this converter are now presented. A stream with an industrial feed composition is introduced through the three inlets of the converter. The inlet temperature is 512 K. The outlet and other temperatures are examined following the convergence of the simulation runs. The temperature profile in the first converter is found to be in close agreement with the industrial one. On the basis of the current simulations, the outlet temperature for this case is found to be 575 K, compared with an industrial value of 572 K.

Figure 10 shows the contours of the main reactant, H_2S. The feed composition of this reactant is 0.06377. The outlet composition is found to be 0.01526, which is 3.7% lower than the actual industrial value of 0.01585.

Most of the SO_2 is consumed at the bed. The inlet composition of SO_2 is 0.06075. When the converged solution is reached, the outlet composition is found to be 0.01515. This is 2% lower than the corresponding industrial value of 0.01485. The fluid distribution in the bed may be more even than that in the industrial case, and this may enhance the production of gaseous sulfur. Another possible reason for the discrepancy between the simulation and the actual results may be related to the life of the catalyst. The simulation assumes fresh catalyst, while the industrial results were reported with a little less active catalyst.

The experimental degree of conversion of SO_2 is found to be 75.5%. This is compared with a predicted conversion of 75.06%. More experimental data is available in the form of temperature readings at nine locations. These locations are inside the bed, three points across the bed below each inlet. The exact locations are specified in the first column of Table 1. The simulation values of temperature are obtained from Figure 11. The

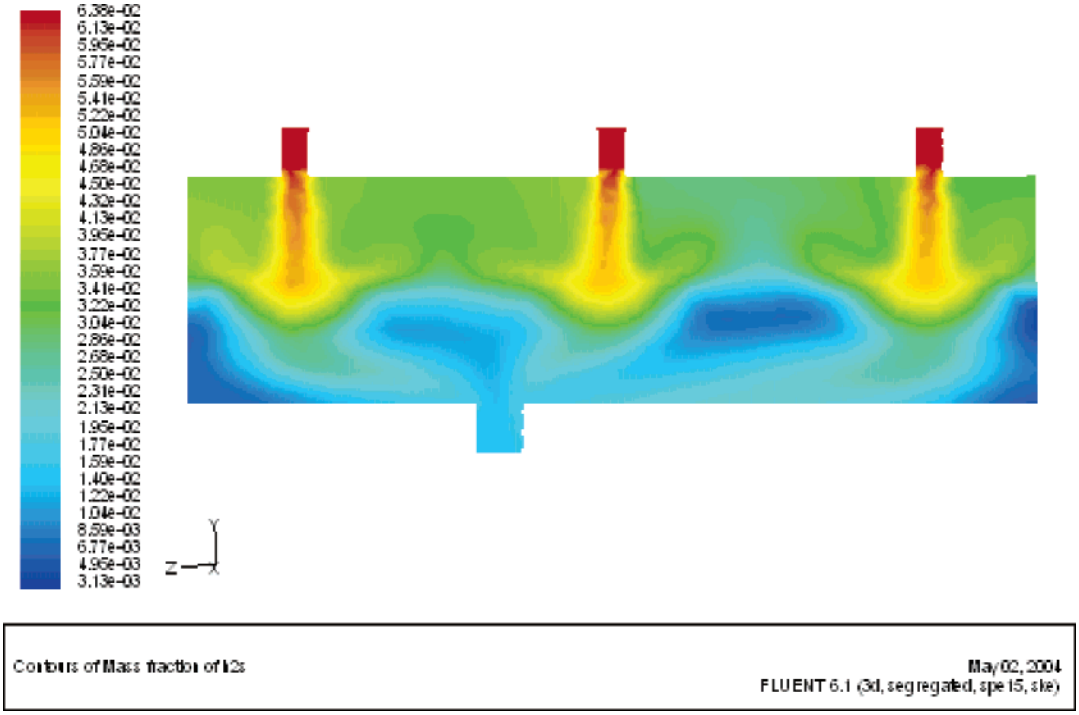

Figure 10. Contours of the H_2S mass fraction in a plane passing through the inlets and the outlet of the first converter.

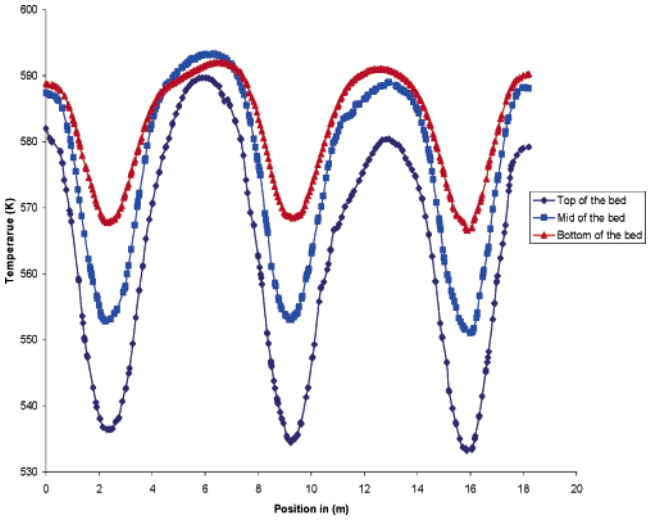

Figure 11. Line plots of the temperature profile at different positions through the catalyst bed in the first converter.

Table 1. Comparison of Predicted and Experimental Temperatures at Identical Locations in the Bed

position (x, y, z)	experimental T (K)	simulation T (K)
(0, −0.15, 2.60)	540	536
(0, −0.15, 10.60)	560	548
(0, −0.15, 16.00)	511	533
(0, −0.60, 2.60)	602	554
(0, −0.60, 10.60)	610	572
(0, −0.60, 16.00)	562	551
(0, −1.05, 2.60)	607	573
(0, −1.05, 10.60)	610	578
(0, −1.05, 16.00)	596	568

temperatures at identical locations to those used for the experiemental data were obtained from the simulation results, and both sets are compared in Table 1.

It can be seen from Table 1 that the simulation results are underpredicting the temperature in the bed except at one point. However, the predicted values of temperature at each of the nine monitoring points show a similar trend to the industrially measured values. A better agreement may be obtained if more accurate kinetics models were used in the simulations.

Table 2. Comparison of the Industrial and Predicted Temperatures and Compositions of the Product Gas

	inlet	outlet	
name	industrial	predicted	industrial
T (K)	511	575	572
H_2S concn	0.06377	0.01527	0.01585
SO_2 concn	0.06075	0.01515	0.01485
H_2O concn	0.044	0.0716	0.07479
S_2 concn	0	0.0113	
S_6 concn	0	0.0213	
S_8 concn	0	0.0401	

Figure 11 shows variations in the values of temperature along three lines. One is near the top (inlet) of the bed, one is near its middle, and one is near the outlet of the bed. This figure shows that the high velocity in the areas of the jet impingement zones plays a major role in reducing the temperature. The zones corresponding to locations between the feed inlets show the highest temperatures. The effects of the velocity on the temperature distribution are further confirmed by noticing that the temperature in the inlet of the bed, where the velocity is high, is much lower than the temperature near the bed outlet, where the velocity becomes better distributed and consequently lower.

The industrial and numerical full compositions of the outlet gas are compared in Table 2. The predicted compositions of H_2S, SO_2, and H_2O are within 4% of the industrial values. The predicted concentrations of S_8, S_6, and S_2 are in close agreement with the values obtained from the equilibrium curves.[15] The industrial measurements do not report the composition of each of S_2, S_6, and S_8. At the relatively low temperature of the converter (compared to the furnace), most of the sulfur vapor produced by the Claus reaction is S_8, followed by S_6 and a trace of S_2. At higher temperatures, such as those in the furnace, S_2 is the dominant species.

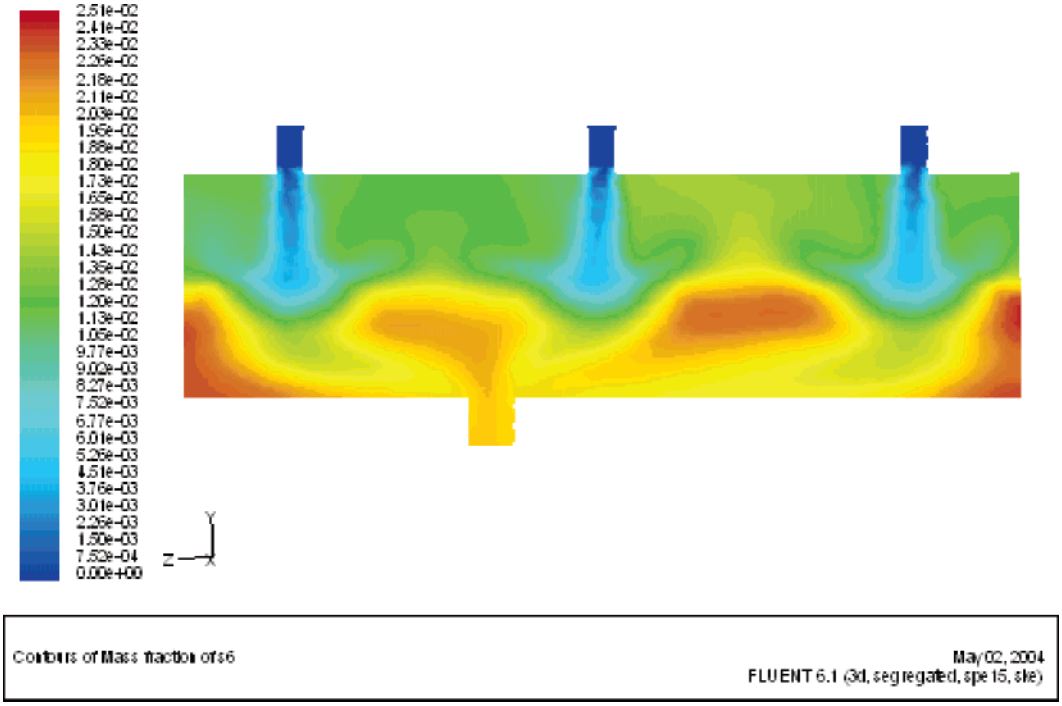

Figure 12. Contours of the S_6 mass fraction in a vertical plane passing through the inlets and the outlet of the first converter.

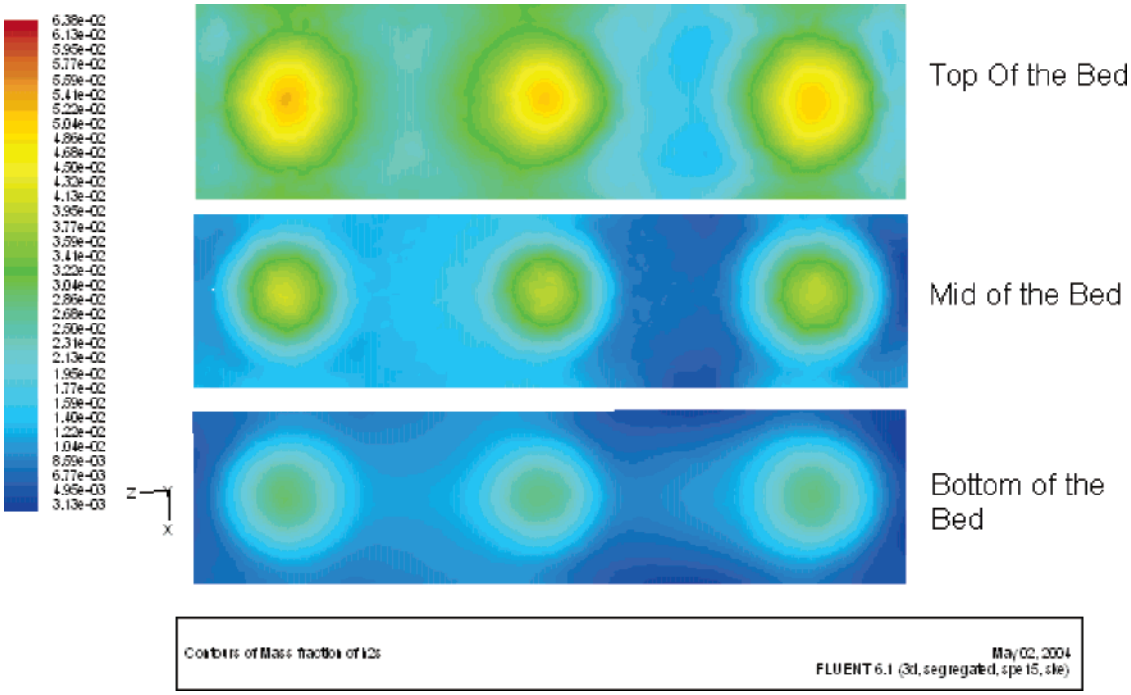

Figure 13. Contours of the H_2S mass fraction in horizontal planes in different positions of the catalyst bed of the first converter.

Table 2 shows that the mass fractions of S_2, S_6, and S_8 are 0.0113, 0.0213, and 0.0401, respectively. Steam is a main product of the Claus reaction. The steam mass fraction in the inlet stream is 0.044 compared to a mass fraction of 0.0716 in the outlet stream. The value reported in the industrial operation is 0.07479. Figure 12 shows contours of the mass fraction of S_6 in a vertical plane passing through the inlets and the outlet of the converter. The mass fractions of S_2 and S_8 show a similar distribution.

Figure 13 shows the contours of the mass fraction of H_2S in three horizontal planes: one near the bottom of the packed bed, one passing through the middle, and one near the top of the bed. This figure clearly shows that conversion is influenced by the velocity and, therefore, mass transfer.

Simulation of Flow, Chemical Reactions, and Heat Transfer in the Second Converter. Following the successful simulation of the flow and chemical reactions in the first converter, the same model of flow and reaction kinetics is now applied to the second converter. The geometry of all three converters used in the Claus process is assumed to be identical. The composition of the feed to the second converter is given in Table 3. This feed is the gas product stream leaving the first converter except for the sulfur vapors, which are condensed and collected before the feed enters the second converter. This typical industrial feed is intro-

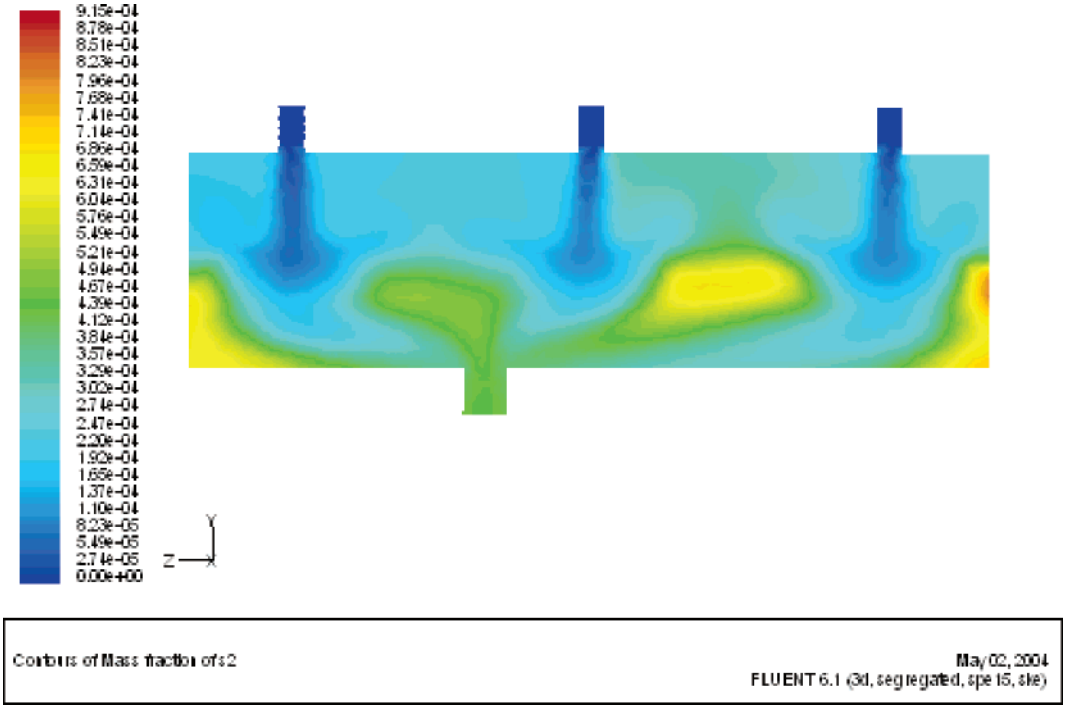

Figure 14. Contours of the S_2 mass fraction in a vertical plane passing through the inlets and the outlet of the second converter.

Table 3. Composition of the Feed to the Second Converter

component	feed composition (mass fraction)
hydrogen	0.0001916
argon	0.003238
nitrogen	0.1898
methane	0.0005494
carbon monoxide	0.001270
carbon dioxide	0.6858
ethane	0.00006599
hydrogen sulfide	**0.01585**
water	0.07479
sulfur dioxide	**0.01485**
carbon disulfide	0.0007292

Table 4. Predicted and Industrially Measured Temperatures at Identical Locations in the Bed of the Second Converter

position (x, y, z)	experimental T (K)	simulation T (K)
(0, −0.15, 2.60)	489.82	491.7
(0, −0.15, 10.60)	489.07	492.82
(0, −0.15, 16.00)	490.21	494.16
(0, −0.60, 2.60)	497.71	493.53
(0, −0.60, 10.60)	498.11	495.25
(0, −0.60, 16.00)	497.71	496.06
(0, −1.05, 2.60)	503.76	491.44
(0, −1.05, 10.60)	503.82	492.40
(0, −1.05, 16.00)	503.37	493.18

duced through the three inlets of the converter. The inlet temperature is 490 K. The flow and chemical reactions are simulated as was done for the first converter.

The predicted outlet temperature for this case is found to be 498 K compared with the industrial value of 501 K. More experimental data is available in the form of temperature readings at nine locations inside the catalyst bed in a vertical plane passing through the inlets and the outlet. These locations are the same as those discussed earlier for the first converter. A comparison of the experimental and predicted temperatures measured at identical locations is shown in Table 4. A reasonable agreement is observed between the experimental and predicted values of the temperature.

Table 5. Comparison of the Industrially Measured and Predicted Temperatures and Compositions of the Product Gas for the Second Converter

	inlet	outlet	
name	industrial	predicted	industrial
T (K)	490	498	501
H_2S concn	0.01585	0.0098	
SO_2 concn	0.01485	0.0092	
H_2O concn	0.07479	0.078	
S_2 concn	0	0.00078	
S_6 concn	0	0.0027	
S_8 concn	0	0.00498	

Figure 14 shows contours of the mass fraction of the S_2 in a plane passing through the inlets and the outlet of the second converter. This S_2 is produced in the bed. The outlet mass fraction of S_2 is found to be 0.00078. The contours of the mass fraction of S_6 and S_8 display a similar distribution. The outlet mass fraction of these compounds is 0.0027 and 0.00498, respectively. This means that 59% of the elemental sulfur leaving the second converter is S_8, 32% is S_6, and the remaining 9% is S_2. The inlet mass fraction of the water vapor is 0.07479, while the outlet composition is 0.078.

According to the equilibrium curves,[15] most of the elemental sulfur produced in the second converter is in fact S_8. At an approximate average temperature of 494 K, the equilibrium composition indicates that S_8, S_6, and S_2 constitute 72%, 26%, and 2%, respectively, of the gaseous sulfur. The differences in the compositions of the sulfur vapors predicted by the present simulations and those deduced from the equilibrium curves are mainly due to kinetics information used in the present simulation.

The mass fraction contours of the reactant SO_2 show a similar trend to those in the first converter. The SO_2 is consumed in the bed, and the distribution within the bed is influenced by the magnitude of the gas velocity. The inlet composition of SO_2 is 0.01485, while the outlet composition is found to be 0.0092. The predicted value of the degree of conversion of SO_2 is 38.07% compared

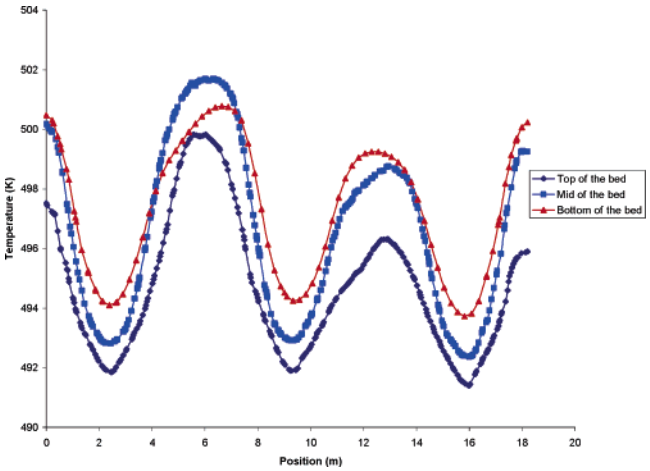

Figure 15. Line plots of the temperatures at different positions of the catalyst bed in the second converter.

to an industrial value of 43.96%. The mass fraction of H_2S in the feed is 0.01585. The predicted mass fraction of H_2S in the product gas is 0.0098.

Table 5 lists the inlet compositions and the predicted outlet results. Table 5 also shows the predicted and industrially measured outlet temperatures. The predicted value is 498 K, while the industrially measured one is 501 K.

Figure 15 shows values of the temperature along three lines in a vertical central ($y-x$) plane passing through the inlets and the outlet of the second converter. The first line is near the inlet of the bed, the second is near the middle of the bed, and the third is near the bed outlet. The trend shows the effects of the high velocity in ensuring a good heat flow. The zones corresponding to those between the incoming jets experience the lowest velocities and have the highest temperatures in the catalyst bed.

Potential Application of the Current Model. Operators of Claus converters are concerned with extending the life of the catalyst. Depending on the feed quality and the type of catalyst used, a Claus converter run could last between 2 and 8 years. No information could be found in the literature that discussed flow maldistribution as a means of enhancing the performance of Claus converters. On the basis of the current results, the design of Claus converters could be modified to ensure a more uniform flow distribution, which in turn ensures better usage of all the regions of the catalyst bed. A better flow distribution could also translate into higher conversion under the same operating conditions or the ability to process higher feed rates.

The design of Claus converters is based on operational rather than process reasoning. The off-center outlet is used for layout purposes, so that the pipes from the converter to the condenser are grouped to one side. CFD modeling could be easily used to test the uniformity of the flow distribution of a modified design of a Claus converter.

Conclusions

The flow, chemical reactions, and thermal effects in Claus catalytic converters were simulated. The feed enters through three inlets and continues as jets until it reaches the catalyst bed. It was found that this catalyst bed acts as a good flow distributor. The maldistribution number defined as (actual velocity − velocity averaged over the bed cross-sectional area)/average velocity is about 28.6 at the inlet of the bed compared with 2.5 near the outlet of the bed. However, some significant differences in the flow velocities were observed in the best part of the packed bed. The flow at the inlet of the bed ranges between 0.2 and 20 m/s, while in the middle of the bed it ranges between 0.2 and 4.5 m/s and near the outlet of the bed it ranges between 0.4 and 1.9 m/s; the velocity averaged over the mid-cross-sectional area is 0.54 m/s. Decreasing the inlet velocity from 57 to 45 m/s or increasing it to 70 m/s did not have any significant effect on the flow distribution inside the converter.

A reaction kinetics model suggested by Abaskuliev et al.[14] was used. This model was adapted to account for the production of S_2, S_6, and S_8. Numerical results showed good agreement with industrially obtained results. The conversion in the first converter was found to be 75.06% compared to an industrial value of 75.5%. The predicted outlet temperature of the first converter was found to be 575 K compared to an experimentally measured value of 572 K. The predicted values of temperature at nine locations inside the catalyst bed were in close agreement with the experimental values.

In the second converter, a similar agreement between simulation and experimental results was also observed. The predicted outlet temperature was found to be 498 K compared to an experimental value of 501 K. The detailed predicted temperature values at nine locations inside the catalyst bed were in good agreement with the experimentally measured temperatures.

This study shows clearly the details of the flow and temperature profiles inside a Claus converter. It opens a window for design improvements which may lead to a better flow distribution and, consequently, to a more even utilization of the catalyst bed. Operators of Claus converters are mainly concerned with extending the life of the catalyst. Close examination of the flow maldistribution may help in doing just that.

Acknowledgment

The authors would like to acknowledge the support of KFUPM (Project ARI-008) during the course of this work and the preparation of this paper. The authors would like to thank Mr. Pierre Crevier of Saudi ARAMCO for his useful comments.

Nomenclature

A_r = pre-exponential factor (consistent units) in the Arrhenius expression
C_2 = inertial resistance factor
$C_{j,r}$ = molar concentration of each reactant and product species j in reaction r (kg mol/m^3)
D_p = diameter of a catalyst particle (m)
E = total energy
E_r = activation energy for the reaction (J/(kg mol))
g = acceleration due to gravity (m^2/s)
J = diffusion flux
h = sensible energy
k_{eff} = effective thermal conductivity
$k_{f,r}$ = forward rate constant for reaction r
$k_{b,r}$ = backward rate constant for reaction r
M_i = symbol denoting species i
N = number of chemical species in the system
N_r = number of chemical species in reaction r
p = pressure (Pa)
N_R = number of reactions

R = universal gas constant (J/(kg mol K))
$\hat{R}_{i,r}$ = Arrhenius molar rate
S_f = source term in the energy equation
S_f^h = source term in the energy equation in porous media
T = temperature (K)
$\bar{v}$ = velocity vector
$\nu'_{i,r}$ = stoichiometric coefficient for reactant i in reaction r
$\nu''_{i,r}$ = stoichiometric coefficient for product i in reaction r

Greek Letters

α = permeability of the catalyst bed
β_r = temperature exponent (dimensionless)
ρ = density (kg/m^3)
μ = viscosity (Pa s)
ϵ = porosity of the catalyst bed
$\eta'_{j,r}$ = forward rate exponent for each reactant and product species j in reaction r (kg mol/m^3)
$\eta''_{j,r}$ = backward rate exponent for each reactant and product species j in reaction r (kg mol/m^3)

Subscripts

f = fluid
s = solid
eff = effective

Literature Cited

(1) Delmas, H.; Froment, G. F. A Simulation Model Accounting for Structural Radial Nonuniformites in Fixed Bed Reactors. *Chem. Eng. Sci.* **1988**, *43*, 2281.

(2) Stanek, V.; Szekely, J. Three-dimensional Flow of Fluids through Nonuniform Packed Beds. *AIChE J.* **1974**, *20*, 974.

(3) Ergun, S. Fluid Flow through Packed Columns. *Chem. Eng. Prog.* **1952**, *48*, 89.

(4) Ziolkowska, I.; Ziolkowski, D. Modeling of Gas Interstitial Velocity Radial Distribution over a Cross-Section of a Tube Packed with a Granular Catalyst Bed. *Chem. Eng. Sci.* **1993**, *48*, 3283.

(5) Bey, O.; Eigenberger, G. Fluid Flow through Catalyst Filled Tubes. *Chem. Eng. Sci.* **1997**, *52*, 1365.

(6) Stanek, V. *Fixed Bed Operations: Flow Distribution and Efficiency*; Ellis Horwood: Chichester, U.K., 1994.

(7) Vortmeyer, D.; Schuster, J. Evaluation of Steady Flow Profiles in Rectangular and Circular Packed Beds by a Variational Method. *Chem. Eng. Sci.* **1983**, *38*, 1691.

(8) Kuipers, J. A. M.; Van Swaaij, W. P. M. In *Computational Fluid Dynamics to Chemical Reaction Engineering*; Wei, J., et al., Eds.; Advances in Chemical Engineering 24; Academic Press: New York, 1998; p 227.

(9) Magnussen. B. F.; Hjertager, B. H. On Mathematical Models of Turbulent Combustion with Special Emphasis on Soot Formation and Combustion. *Symp. (Int.) Combust., [Proc.]* **1976**, 16.

(10) Jiang, Y.; Khadilkar, M. R.; Al-Dahhan, M. H.; Dudukovic, M. P. Single Phase Flow Distribution in Packed Beds: Discrete Cell Approach Revisited. *Chem. Eng. Sci.* **2000**, *55*, 1829.

(11) Jiang, Y.; Khandilkar, M. R.; Al-Dahnan, M. H.; Dudukovic, M. P. CFD of Multiphase Flow in Packed-Bed Reactors: I. *K*- Fluid Modeling Issues. *AIChE J.* **2002**, *48*, 701.

(12) *Fluent User Guide*; Fluent Incorporation: 2003.

(13) Monnery, W. D.; Hawboldt, K. A.; Pollock, A.; Svreck, W. Y. New Experimental Data and Kinetic Rate Expression for the Claus Reaction. *Chem. Eng. Sci.* **2000**, *55*, 5141.

(14) Abaskuliev, D. A.; Guseinov, N. M.; Mekhraliev, A. Ch. Mathematical Model of the Catalytic Convertor of a Claus Unit. *Gazov. Promst.* **1990**, *9*, 60.

(15) Maddox, R. N. In *Gas and Liquid Sweetening*; Campbell, J. M., Ed.; Campbell Petroleum Series: Norman, OK, 1974.

(16) Szkely, J. L.; Poveromo, J. J. Flow Mal-distribution in Packed Beds: A Comparison of Measurements with Predictions. *AIChE J.* **1975**, *21*, 769.

Received for review April 2, 2005
Revised manuscript received August 31, 2005
Accepted September 28, 2005

IE050412M